DEPARTMENT OF PHYSICS
UNIVERSITY OF JYVÄSKYLÄ
RESEARCH REPORT No. 2/2001

THE MECHANICAL AND GEOMETRICAL PROPERTIES OF FIBROUS STRUCTURES

BY
JUKKA MÄKINEN

Academic Dissertation
for the Degree of
Doctor of Philosophy

Jyväskylä, Finland
April 2001

DEPARTMENT OF PHYSICS,
UNIVERSITY OF JYVÄSKYLÄ
RESEARCH REPORT No. 2/2001

THE MECHANICAL AND GEOMETRICAL PROPERTIES OF FIBROUS STRUCTURES

BY
JUKKA MÄKINEN

Academic Dissertation
for the Degree of
Doctor of Philosophy

To be presented, by permission of the
Faculty of Mathematics and Natural Sciences
of the University of Jyväskylä,
for public examination in Auditorium FYS-1 of the
University of Jyväskylä on May 11, 2001
at 12 o'clock noon

Jyväskylä, Finland
April 2001

URN:ISBN:978-951-39-9493-8
ISBN 978-951-39-9493-8 (PDF)
ISSN 0075-465X

ISBN 951-39-0895-X
ISSN 0075-465X

Preface

The studies reviewed in this thesis were carried out during the years 1996-2000 in the Department of Physics at the University of Jyväskylä. I express my gratitude to my supervisor, Prof. Jussi Timonen for his patience and fatherly advice throughout the years. I am very much indebted to Dr. Jan Åström without whom, I fear, most of the articles included in this thesis would not have materialised. To my friends at FL348, I owe my sanity.

Helsinki, 1 April 2001

Jukka Mäkinen

Abstract

This thesis deals with both random and regular (woven) fibre networks. An effective medium theory for the tensile stiffness of two-dimensional random fibre networks is presented. The theory is extended to three-dimensional networks with some but not too strong restrictions. This generalisation involves the computationally determined fraction of bonded crossings in the two-dimensional projection of the three-dimensional network. The two-dimensional and three-dimensional versions of the theory are both succesfully tested against numerical simulations.

The porosity of the three-dimensional random fibre networks is found to be given by a numerically determined scaling function, which upon rescaling is shown to be similar to the fraction of bonded crossings described above. This function thus seems to determine the entire structure and mechanical behaviour of randomly deposited fibre mats.

A numerical model for the mechanical equilibration of woven fibre networks is also presented. Structures generated by this model are tested against industrially manufactured fabrics. This comparison shows that the model gives fairly realistic results, which guarantees its usefulness also in industrial applications.

List of publications

I Elasticity of Poissonian Fiber Networks
J.A. Åström, J.P. Mäkinen, M.J. Alava, and J. Timonen
Phys. Rev. E **61**, 5550 (2000)
https://doi.org/10.1103/PhysRevE.61.5550

Ia Erratum: Elasticity of Poissonian Fiber Networks
J.A. Åström, J.P. Mäkinen, M.J. Alava, and J. Timonen
Phys. Rev. E **62**, 5862 (2000)
https://doi.org/10.1103/PhysRevE.62.5862

II Stiffness of Compressed Fiber Mats
J.A. Åström, J.P. Mäkinen, H. Hirvonen and J. Timonen
J. Appl. Phys. **88**, 5056 (2000)
https://doi.org/10.1063/1.1315622

III Elasticity and Porosity of Three Dimensional Mats of Randomly Deposited Fibers
J.P. Mäkinen, J.A. Åström, S. Kähkönen and J. Timonen
Submitted.
https://doi.org/10.1007/s10035-003-0131-0

IV Modeling Multilayer Woven Fabrics
J.A. Åström, J.P. Mäkinen, and J. Timonen
Submitted.
https://doi.org/10.1063/1.1385350

V A Relaxation Model for Multi-Layered Woven Fabrics
J.P. Mäkinen, J.A. Åström and J. Timonen
Proceedings of ECCOMAS 2000 (2000)

The author's contribution

The author of this thesis wrote the first drafts of the papers [III] and [V], and selected parts of the papers [II] and [IV]. The author did almost all of the numerical work and participated in the development of the analytical models.

Contents

1 Introduction

A fundamental problem in condensed matter physics is to understand the macroscopic properties and the structure of systems of particles in terms of the interparticle interactions [1]. Most of materials research is done in the molecular scale, although for many materials there are much larger length scales that are as well important for their mechanical behaviour. This thesis concentrates on the study of mechanical and geometrical properties of three-dimensional regular and disordered fibrous materials. Early studies in the physics of disordered fibrous materials mainly considered the percolation problem [2, 3, 4] or fracture [5], while their structural and elastic properties were mostly considered in engineering sciences [6, 7].

The concept of disorder gives a feeling that there is something that falls short of the ideal of order [8]. Order is a rule that defines the system perfectly whereas disorder implies randomness. However, a disordered system can still have order in it, and this partial order usually makes a difference. In industrial applications the demand for controlling the scales of disorder is growing as the materials are being optimised for various end-use requirements. This induces a need to understand the charasteristics of disordered materials. Industrially manufactured fibrous materials are formed as regular or random networks, from both of these an example is presented in this thesis. Examples of this kind of materials range from insulator materials and glass-fibre felts to short-fibre composites and paper.

To begin with the basics of elasticity theory, and of the computational methods used, are introduced in the following Section 2. Thereafter the developed effective-medium (EM) model for the tensile stiffness of materials composed of randomly connected building blocks is presented. The EM model is tested against a numerical model that is also described in detail. The basic idea of the EM model, applied here can also be applied to other systems of randomly connected building blocks but this extension of the model is not considered here. The geometry of the random fibre network is then studied in terms of its porosity, which leads to a function we call the *process function*. This function seems to determine the entire structure and the mechanical behaviour of random fibre networks.

The rest of the thesis deals with regular woven (fibrous) structures. A numerical model for relaxing a woven system to its elastic equilibrium is introduced. This model employs a version of the gradient method, and seems to give realistic results when compared visually with real fabrics. The model has obvious applications in industry where different fabric structures are constantly being designed for optimum fluid permeability, durability and stiffness, just to mention a few examples of their desired functional properties.

2 Elasticity

The mechanics of solid bodies, regarded as continuous media, forms the content of elasticity theory. The basic equations of the theory date back to the 1820's, to the work by Cauchy and Poisson. As this thesis incorporates elasticity theory in the analytical as well as in the simulation models, the fundamental equations of the theory are briefly mentioned. The solution methods used in the computer implementations are also derived.

2.1 Fundamental equations

The strain tensor u_{ik} is defined through the derivatives of the displacement vector u_i [9] such that

$$u_{ik} = \frac{1}{2}\left(\frac{\partial u_i}{\partial x_k} + \frac{\partial u_k}{\partial x_i} + \frac{\partial u_l}{\partial x_i}\frac{\partial u_l}{\partial x_k}\right), \tag{1}$$

where the third term on the right side can be left out for small deformations.

For homogeneous deformations the stress tensor in terms of the strain tensor is given by

$$\sigma_{ik} = \frac{E}{(1+\sigma)}\left(u_{ik} + \frac{\sigma}{1-2\sigma}u_{ll}\delta_{ik}\right), \tag{2}$$

where E is the Young's modulus and σ is the Poisson ratio. Conversely,

$$u_{ik} = [(1+\sigma)\sigma_{ik} - \sigma\sigma_{ll}\delta_{ik}]. \tag{3}$$

For isotropic bodies the equilibrium condition can be expressed in the form

$$(1-2\sigma)\frac{\partial^2 u_i}{\partial x_k^2} + \frac{\partial^2 u_l}{\partial x_i x_l} = 0. \tag{4}$$

The possible external forces appear in the solution only through the boundary conditions.

2.2 Rigid bodies

For a simple extension or a compression of a body we get, from Eqs. (2) and (3),

$$\sigma_{xx} = Eu_{xx}, \tag{5}$$

where elongation is along the x-axis. If the Poisson contraction is prohibited in the y-direction, we get from the same equations

$$\sigma_{xx} = \frac{E}{(1-\sigma^2)}u_{xx}. \tag{6}$$

For a shear deformation of a body we get, again from Eqs. (2) and (3),

$$\sigma_{xy} = \frac{E}{2(1+\sigma)}u_{xy}. \tag{7}$$

2.3 Rigid rods

The basic building blocks of the models presented in [I, Ia, II, III] are linear elastic rods with a square cross-section.

From the Eq. (5) we get for the elongation of a rod along the x-axis

$$x = \frac{l}{EA} F_x, \tag{8}$$

where l is the length of the rod, A is the cross-section, x is the displacement of the other end of the rod with one end clamped, and F_x is the related force.

For the bending of a rod it is easier to start from the relative change in a differential element of the rod than from the equations mentioned above. This means that

$$\frac{\Delta ds}{ds} = \frac{y_1}{r}, \tag{9}$$

where the element $ds + \Delta ds$ is at the distance of $r + y_1$ from the centre of curvature of the element, and r is the radius of curvature, see Fig. 1.

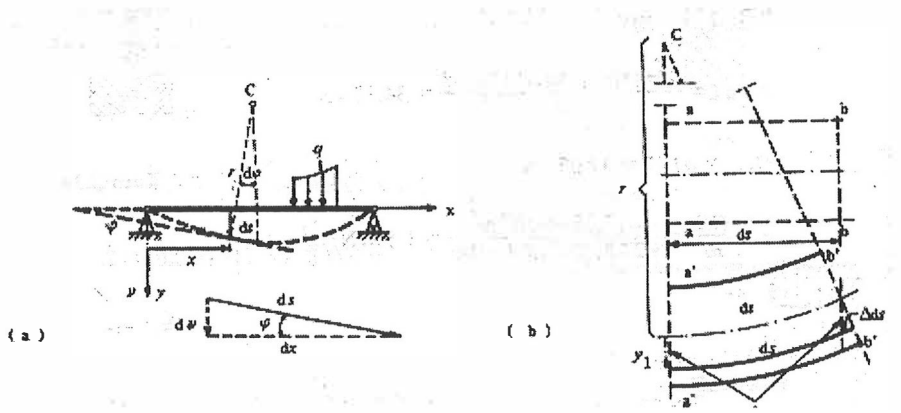

Figure 1: The change in the element of length of a bent rod. [E. Pennala, Lujuusopin perusteet, Otakustantamo 407, Helsinki 1990]

Remembering that

$$u_{xx} = \frac{\Delta ds}{ds} = \frac{\sigma_{xx}}{E} = \frac{M}{EI_z} y_1, \tag{10}$$

we get

$$\frac{1}{r} = \frac{M}{EI_z}, \tag{11}$$

where I_z is the momentum of inertia of the rod and M is the moment inflicted at the rod. From simple geometry[1] we get

$$\frac{1}{r} = \frac{\frac{d^2y}{dx^2}}{[1 + \left(\frac{dy}{dx}\right)^2]^{3/2}}, \tag{12}$$

[1]Since, $ds = -rd\phi$, $dx = \cos\phi ds$ and $tan\phi = \frac{dy}{dx}$, we get $\frac{1}{\cos^2\phi} = \frac{d^2y}{dx^2}$. Realising that $-\frac{1}{r} = \cos^3\phi \frac{d^2y}{dx^2}$, and using $\cos^3\phi = (1 + tan^2\phi)^{-3/2}$, Eq. (12) follows.

which, since dy/dx is small, can be linearised to give

$$\frac{1}{r} = -\frac{d^2y}{dx^2}. \tag{13}$$

Using Eq. (11) we arrive at the differential equation [9, 10]

$$EI\frac{d^2y}{dx^2} + M(x) = 0, \tag{14}$$

where I is the momentum of inertia of the rod and $M(x)$ is the moment inflicted at the point x of the rod. This equation describes the line of bending for the rod assuming that bending takes place in the xy-plane. From this one can find the solution for two relevant cases. For bending of one end with the other end clamped, we get [10]

$$\Omega = \frac{Ml}{4EI}, \tag{15}$$

where Ω is the angle of rotation of the other end of the rod, and M is the related moment. For a pure transverse translation of one end with the other end clamped, we get [10]

$$y = \frac{F_y l^3}{12EI}, \tag{16}$$

and

$$y = \frac{Ml^2}{6EI}, \tag{17}$$

where y is the displacement of the other end of the rod, F is the related force and M is the related moment.

2.4 Multi-element systems

When an elastic body is at equilibrium its every part is at equilibrium. This means that no matter what part we cut out of the body, that part can be thought of as being an independent body at equilibrium with the boundary conditions imposed by the surrounding parts. It is no wonder then that the birth of the theory of finite elements took place in the field of structural analysis. Since its early years in the 1950's in aircraft industry, the theory of finite elements has evolved into a sophisticated mathematical theory for solving partial differential equations [11, 12, 13, 14, 15, 16].

The FEM-procedure can be specified as follows [17]. One starts by variationally formulating the partial differential equation describing the problem[2]. The area considered is discretised by setting the element mesh, element types and the boundary conditions. From the variational formulation we get a linear system of the type

$$\mathbf{F} = K\mathbf{U}, \tag{18}$$

which can be solved using one of the many solution methods for groups of linear equations, see Section 2.5 for references and examples. The solution can then be postprocessed for error estimation and visualisation.

[2]It should be noted that the variational method works only if the variational form exists, *i.e.*, the differential operator related to the equation is both linear and self-adjoint. Another, more general method, is the method of weighted residuals.

In network structures the division into elements is quite natural. The more or less pointlike connections between fibre segments in the network correspond to the pointlike connections between elements in the finite element method. Therefore, while generally the finite element method is approximative, the result in network applications is usually very accurate.

In [I, Ia] the network is two-dimensional and the fibre-fibre bonds have three degrees of freedom: two translations and a rotation. For a single segment along the x-axis, the elastic interaction between its ends can be defined using the relations Eqs. (8), (15), (16) and (17) in the form of a stiffness matrix

$$K_1 = \begin{pmatrix} \frac{EA}{l} & 0 & 0 & -\frac{EA}{l} & 0 & 0 \\ 0 & \frac{12EI}{l^3} & \frac{6EI}{l^2} & 0 & -\frac{12EI}{l^3} & \frac{6EI}{l^2} \\ 0 & \frac{6EI}{l^2} & \frac{4EI}{l} & 0 & -\frac{6EI}{l^2} & \frac{2EI}{l} \\ -\frac{EA}{l} & 0 & 0 & \frac{EA}{l} & 0 & 0 \\ 0 & -\frac{12EI}{l^3} & -\frac{6EI}{l^2} & 0 & -\frac{12EI}{l^3} & \frac{6EI}{l^2} \\ 0 & \frac{6EI}{l^2} & \frac{2EI}{l} & 0 & -\frac{6EI}{l^2} & \frac{4EI}{l} \end{pmatrix}. \tag{19}$$

The stiffness matrix K_1 must be multiplied with the displacement vector (x_1, y_1, Ω_1, x_2, y_2, Ω_2) to obtain the forces acting on the bonds at the segment ends, c.f. Eq. (18). If the segment is in some other angle, the stiffness matrix as well as the force vector and the displacement vector must be rotated using the rotation matrix T (with transpose $\tilde{T}$), and we get for the stiffness matrix

$$K_1' = \tilde{T} K_1 T, \tag{20}$$

while the force vector is given by

$$F_1' = \tilde{T} F_1, \tag{21}$$

and the displacement vector by

$$U_1' = \tilde{T} U_1. \tag{22}$$

The global displacement and force vectors consist of all the local displacement and force vectors. The global stiffness matrix is then constructed by summing up the local stiffness matrix elements of the corresponding degrees of freedom. Generalisation to three dimensions is straightforward, being a simple procedure of increasing the degrees of freedom.

2.5 Solution methods for the elastic equations

The finite element method incorporates a solution of a sparse set of linear equations which is the most time consuming part of the method. Solution methods for sets of linear equations [18] are divided into direct [19, 20] and iterative methods [21, 22]. Direct methods are based on Gauss elimination. Iterative methods are often faster than their direct counterparts but are also more difficult to use. They involve an initial guess from which the system is iterated until the desired accuracy is achieved. These methods rarely change the matrix making them well suited for sparse systems. In the following the two iterative solution methods used in this work are briefly described.

2.5.1 Conjugate gradient method

The solution of Eq. (18) can be found by minimising

$$f(\mathbf{U}) = \frac{1}{2}\tilde{\mathbf{U}}K\mathbf{U} - \tilde{\mathbf{F}}\mathbf{U} + \mathbf{c}. \tag{23}$$

As the stiffness matrix K is both symmetric and positive definite, the minimum is found at the point where

$$\nabla f(\mathbf{U}) = K\mathbf{U} - \mathbf{F} = \mathbf{0}. \tag{24}$$

The system is iterated using

$$\mathbf{U}^{k+1} = \mathbf{U}^k + \alpha_k \mathbf{p}^k, \tag{25}$$

where α_k are chosen such as to minimise $f(\mathbf{U}^{k+1})$, and the optimisation direction is conjugated to the matrix K, *i.e.* $< \mathbf{p}^i, K\mathbf{p}^j >= 0$, for $i \neq j$.

The method is often used in solving large sets of linear equations. Explicit algorithms [23, 24, 25] and well tested libraries [26, 27, 28, 29] are readily available. In [I, Ia, II, III] we used the conjugate gradient subprogram found in the NAG-library.

2.5.2 Pull-detect method

The deformations in [I, Ia, II, III] were considered infinitesimal, which lead us to the linear equation (18) and linear solvers like the conjugate gradient method explained in Section 2.5.1 above. In [IV, V] we faced the problem of finding the elastically relaxed state of a woven structure. The approach chosen was to start from an initial configuration and then letting the system find its way to the elastic equilibrium by pulling at the fibres at the periodic boundaries. This implies moving the contacts formed between the fibres towards the local elastic equilibria as the strain propagates to the network from the boundaries. By forcing finite deformations, discontinuities are introduced in the derivatives of the elastic response functions of the system as new contacts are formed and old ones are opened up [IV, V] In solving the problem we employed the gradient method for temporally variable problem sizes. The direction vector $\mathbf{p}_c^k$ for a single contact is given by

$$\mathbf{p}_c^k = \sum_{neighbours} t_n \mathbf{l}_\mathbf{n}, \tag{26}$$

where $\mathbf{l}_\mathbf{n}$ is the unit vector at the contact in the direction of the n^{th} neighbouring segment, and t_n the tension at the n^{th} neighbouring segment. The size of the problem, *i.e.* the size of the vector $\mathbf{U}$ containing the contact coordinates and the size of the direction vector $\mathbf{p^k}$ holding the iterative directions of all the contacts, vary during the iterations as new contacts are formed and old ones are opened up. The structure is assumed to be elastically relaxed when the contact motions are below some preset limit.

3 Random fibre networks

3.1 Brief review

In nature, organic materials composed of fibres in more or less random positions and angles often result from a huge optimisation process called evolution. A good example of this kind of material is bone that is constructed of fibres and lamellae in optimised angles and positions to serve the purpose of any specific bone. As random fibrous materials offer a good strength over weight ratio in addition to a relatively easy manufacturing process, the understanding of these materials is important also from the industrial point of view. Materials of this kind include glass-fibre felts and paper. The question is how to change the properties of the constituents in order to get a desired property in the material as a whole.

Both academic and industrial interests have induced several studies on the matter. Studies span from connectivity and wave propagation [30, 31, 32, 33] to rigidity [34, 35, 36] and fracture dynamics [37, 38], and from deposition models to lattices with disorder.

Lattices are regular structures composed of *e.g.* triangles, squares or hexagons. These structures can then be perturbed by moving the lattice sites such that the site changes are governed by a distribution. As an example, the stress distribution of a perturbed regular network shown in Fig. 2 was studied by Rigdahl *et al.* [39] by means of finite element simulations. The fibres were in this study modelled as linearly elastic straight beam elements. One of the results of this study was that the strain on a fibre is zero at the ends but away from the ends rises quickly to a plateau, with a maximum if and where a neighbouring fibre is "broken". Also, the bond stiffness was found to be of small importance unless it is below some critical value, in which case the strain transfer deteriorates rapidly.

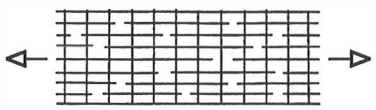

Figure 2: Sketch of the Rigdahl *et al.*'s network geometry [39].

Deposition models constitute a class of methods that have been used to create random fibre structures. The geometry of the structure can then be analysed for different purposes and under varying conditions. The deposition model used in this thesis was first proposed in 1991 by Hamlen [6]. In his ***sequential deposition*** model the fibres were deposited on top of the previously deposited fibres, and given a possibility to bend a 'limit angle' on contacts with the fibres below, possibly coming in contact this way with yet more fibres. The fibre-to-fibre contacts were modelled as beam elements, and numerical computations resulted in a notion that the dominant mode of deformation is elongation of the fibres, which leads to shear forces on the contacts.

In estimating the elastic properties of inhomogeneous materials one usually considers a representative volume element and its response to mechanical perturbations in the mean-field sense. This usually works if the structure of the

material is simple enough. A mean-field theory for the mechanics of fibre networks was introduced by Cox [40] in 1952. Both two- and three-dimensional networks were studied. In two dimensions Cox' network consists of long thin straight fibres extending from one edge of the network to another with a random orientation distribution, see Fig. 3. The bending stiffness of the fibres is thought to be negligible. Also, there is no interaction between the fibres. Instead, the strain field is assumed to be homogeneous throughout the network. For an isotropic fibre orientation distribution the Cox-model gives for the Young's modulus of the network, *i.e.* for the Young's modulus per unit thickness in this case of a 2D network,

$$E = \frac{1}{3} E_f A_f \rho, \tag{27}$$

where E_f is the Young's modulus of the fibres, A_f is the cross-sectional area of the fibres and ρ is the total fibre length per unit area.

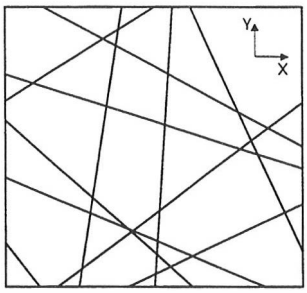

Figure 3: Cox' homogeneous network.

In the shear-lag model [41] the fibres are of finite length. The attachment of a fibre to the elastic sheet, that is, to the rest of the network, is via the nearest segments of the crossing fibres, see Fig. 4. This way the model assumes a shear-lag mechanism in which the stress of a matrix is gradually transferred to a fibre so that the stress is largest in the middle and reduces towards the ends of the fibre. The elastic modulus given by the shear-lag model is

$$E = \frac{3}{8} E_f A_f (\rho - \frac{\pi \rho_c}{5.71} \sqrt{1+\nu}), \tag{28}$$

where $\rho_c = 5.71/L_f$ is the average density required to obtain a mechanically connected random fibre network [2] for an infinitely sized system. The second term on the right side of Eq. (28) is due to the stress vanishing at the ends of the finite length fibres, and is thus a direct consequence of the assumed stress transfer mechanism.

Computer simulations [42, 43, 44] reveal that the Young's modulus (E_e) of the fibre network is asymptotically a linear function of the areal mass density ρ_m such that

$$E_e(\rho_m) = A(\rho_m - \rho_{m0}), \tag{29}$$

where ρ_{m0} and A are constants. Summarizing, also the shear-lag model based on the Cox-model , produces a relation like Eq. (29), with however a ρ_{m0} that

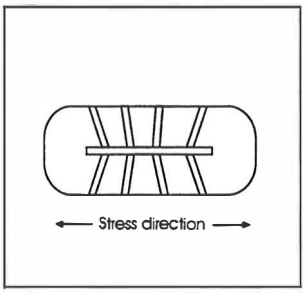

Figure 4: Connection of a fiber to the elastic sheet in the shear-lag model.

is a function of L_f, which is not supported by experiments on paper sheets [45]. Also, the value obtained for ρ_0 is much smaller than in reality, and the value of the modulus A is reproduced, at best, qualitatively [42, 45].

We have therefore introduced a new effective medium model, in which we have however preserved the seemingly correct [43, 44] displacement field. The stress-transfer mechanism assumed by the Cox and the shear-lag model does not seem to be correct [42, 46, 47], and we do not apply it. Instead of the fibre, the basic building block in our model is the fibre segment. The basic argument is that the network spontaneously tries to minimise its elastic energy by locally choosing the segment deformation mode of lowest elastic resistance. A two-dimensional model for the tensile stiffness of the random fibre networks is thus presented along with a generalization of the model to three dimensions, through a bonding fraction that characterises the planar projection of the three-dimensional fibre network. The porosity of three-dimensional random fibre network can also be studied with this effective medium model. The analytical model is tested against a numerical deposition model of two- and three-dimensional random fibre mats.

3.2 Numerical deposition model

In the two-dimensional fibre deposition model the fibres are dropped vertically on a planar substrate with their positions and in-plane angles randomised. By treating the fibre crossings as rigid contacts, a nearest-neighbour network is built. A two-dimensional fibre network generated in this way is shown in Fig. 5.

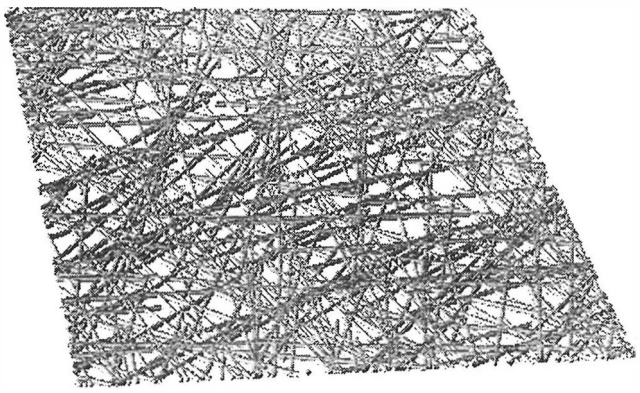

Figure 5: A two-dimensional random fiber mat, $q/q_c = 10$. The number of fibres in the network is on the average qL_xL_y/L_f^2, where q is the dimensionless fibre density, L_xL_y is the area of the network and L_f is the length of a fibre. For a network of infinite size at its connectivity percolation limit, $q_c \approx 5.7$ [2]. The two densities used here, q and ρ, are related as $q = \rho L_f$.

In the three-dimensional model the fibres are dropped vertically as in the two-dimensional model. However, as the density of the mat increases, the fibres start falling on top of each other. Upon contact a contact-node is created on both fibres two fibre radii apart. The upper fibre is then allowed to bend an angle ϕ on both sides of the lower fibre. As the fibre is bent, it may come in contact with the fibres below, in which case another contact-node-pair is created, and the fibre bends in the other direction in between the two contact-node pairs, *i.e.* a bending node is formed there. If the fibre touches the substrate, a bending-type node is created at the point of contact whereafter the fibre lies flat on the substrate. At the ends of the fibres an end-node is created, and these are left hanging at angle ϕ. The effect of the bending angle is shown in Fig. 6.

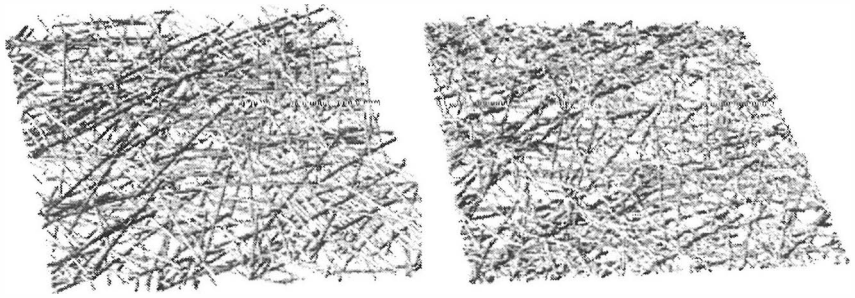

Figure 6: Three-dimensional random fiber mats with $q/q_c = 10$, $L_f = 1.0$, and fibre width $w = 0.2$, for $\phi = 0.1rad$ (left) and $\phi = 0.5rad$ (right).

By identifying the two nodes of a fibre-fibre-contact, a nearest neighbour network is built, which uniquely defines the network. The segments between the nodes of different types are assumed to be linear-elastic rods with a square

cross-section w^2 and length l. Young's modulus is set to unity, and the Poisson ratio is zero. The fibre-to-fibre contacts are assumed rigid in both two- and three-dimensional fibre networks. The stiffness matrix is then constructed as explained in Section 2.4.

Elastic properties of the random fibre networks are analysed by applying external forces at the left and right boundaries of the network, while periodic boundary conditions are imposed in the transverse in-plane direction. A deformation in the networks is created such that the boundary nodes at the right boundary are forced to move a unit distance in the desired direction, while the nodes at the left boundary are forced to stay at their original positions. The equilibrium configuration of the deformed fibre structure is found by using a conjugate-gradient method. From that the appropriate elastic constants can be deduced.

The porosity of a three-dimensional random fibre network is analysed by determining the plane porosity, which we define as the fraction of a cross-section of the network not covered by fibres, for a suitably dense set of in-plane cross sections. Since the fibres cross each cross section at the same angle ϕ, we only need to count the number of crossing fibre segments. The area blocked by the segments is then simply this number times the area, $A_f = w^2/\sin\phi$.

3.3 Effective-medium model

The elastic energy of a fibre mat is found by summing up the elastic energies of the fibre segments in the mat. The basic argument of the effective-medium model introduced here is that the segments will deform in a way that offers the least local elastic resistance in response to the global strain. In the following the elastic energies of the single segments in response to the total deformation of the mat are specified. As defined in Section 2.4, where $A = w^2$, the elongation-stiffness modulus is Ew^2/l, the bending-stiffness modulus is Ew^4/l^3 and the shear-stiffness modulus is $Ew^2/[2(1+\nu)l]$. Assuming now that a segment deforms only by bending, if the bending modulus is smaller than both the shear and the elongation modulus, we get a crossover length $l_c \equiv w\sqrt{2(1+\nu)}$.

The elastic energy of a segment is of the form $W = \frac{1}{2}Kx^2$, where K is the string constant, *i.e.* the stiffness, and x is the displacement of one end of the segment while the other end is kept immobile. For a segment at an angle θ to the direction of the strain ϵ_x, the displacement is $x = \epsilon_x l\cos\theta$. The axial displacement is therefore $\epsilon_x l\cos^2\theta$, and the transverse displacement is $\epsilon_x l\cos\theta\sin\theta$. For a single segment the elastic energy of a bending deformation is thus

$$W^{bnd}(\theta) = \frac{1}{2}\frac{Ew^4}{l^3}\left(\epsilon_x l\cos\theta\sin\theta\right)^2. \tag{30}$$

Similarly the elastic energy of a stretched segment is

$$W^{str}(\theta) = \frac{1}{2}\frac{Ew^2}{l}\left(\epsilon_x l\cos^2\theta\right)^2, \tag{31}$$

and that of a sheared segment

$$W^{shr}(\theta) = \frac{1}{2}\frac{Gw^2}{l}\left(\epsilon_x l\cos\theta\sin\theta\right)^2, \tag{32}$$

where $G = E/(2(1+\nu))$.

The number of fibres in the network is qL_xL_y/L_f^2, where as before L_xL_y is the planar area of the net, L_f is the length of a fibre, and q is the average number of fibres in the area of size L_f^2; q relates to the fibre density ρ used in Section 3.1 as $q = \rho L_f$. Multiplying this with the average number of segments on a fibre $L_f/\hat{l}$, we get the average number of segments in the network,

$$N = \frac{qL_xL_y}{L_f^2}\frac{L_f}{\hat{l}}, \tag{33}$$

where $\hat{l} = \frac{L_f\pi}{2aq}$ is the average segment length in the system. If only a randomly chosen fraction of the fibre crossings is bonded, the average segment length will increase. This increase is described by the parameter a, *i.e.* the *fraction of bonded crossings*, by which $\hat{l}$ should be divided. The segment lengths are distributed like in a one-dimensional Poisson process which leads to the length distribution [I]

$$\mu(l) = \hat{l}^{-1}exp\left(-\hat{l}^{-1}l\right), \tag{34}$$

where the parameter a can be introduced, as it only changes the frequency of the Poisson process, through the average segment length $\hat{l}$.

To get the elastic energy of the whole network in two dimensions, we must sum up the energies of the different deformation modes. The energies of the respective modes are calculated by multiplying the energy of the single-segment deformation (Eqs. (30),(31),(32)) by the average number of such segments, and then integrating over the segment length distribution with appropriate limits. The elastic energy of the whole network is then given by

$$\begin{aligned}
W = &\frac{Ew^2}{2}\epsilon_x^2 q\frac{L_xL_y}{L_f}\int_{-\frac{\pi}{2}}^{\frac{\pi}{2}}\frac{\cos^4(\theta)}{\pi}d\theta\int_0^{l_c}(\frac{2aq}{\pi L_f})^2 le^{(\frac{-2aql}{\pi L_f})}dl \\
&+\frac{Gw^2}{2}\epsilon_x^2 q\frac{L_xL_y}{L_f}\int_{-\frac{\pi}{2}}^{\frac{\pi}{2}}\frac{\cos^2(\theta)\sin^2(\theta)}{\pi}d\theta\int_0^{l_c}(\frac{2aq}{\pi L_f})^2 le^{(\frac{-2aql}{\pi L_f})}dl \\
&+\frac{Ew^4}{2}\epsilon_x^2 q\frac{L_xL_y}{L_f}\int_{-\frac{\pi}{2}}^{\frac{\pi}{2}}\frac{\cos^2(\theta)\sin^2(\theta)}{\pi}d\theta\int_{l_c}^{\infty}(\frac{2aq}{\pi L_f})^2 l^{-1}e^{(\frac{-2aql}{\pi L_f})}dl,
\end{aligned} \tag{35}$$

where the energies of the deformations by stretching, shearing and bending are represented by the first, the second and the third term on the right side, respectively.

3.4 Results

3.4.1 stiffness

The behaviour of the deformed segments is of course more complex than the assumption made above of having only the leading deformation mode. The actual deformations incorporate all the modes but the assumption becomes somewhat more realistic if we treat the crossover length l_c as a fitting parameter. From the simulations [I, Ia] we find that

$$l_c = (1.6w + 0.11)\sqrt{2(1+\nu)} \tag{36}$$

gives a fairly good agreement between the effective-medium model and the numerical simulations.

By solving the integrals in Eq. (35) and using $W = (1/2)E_e e_x^2 L_x L_y$, we get the elongation stiffness of a two-dimensional random fibre mat in the form

$$E_e = \frac{Ew^2 q_l}{8L_f}\left[\left(\frac{2aqw}{\pi L_f}\right)^2 E_1(z) + \left(3 + \frac{1}{2(1+\nu)}\right)(1 - e^{-z}(z+1))\right], \quad (37)$$

where z is now $z \equiv 2aql_c/(\pi L_f)$ and $E_n(z) \equiv \int_1^\infty \frac{e^{-zx}}{x^n} dx$ is the Exponential-Integral function, and cannot thus be expressed in terms of elementary functions. It can, however, be approximated by a rational approximation, Eq. (6) in Refs. [I, Ia], to give a universal one-parameter form for the mat stiffness,

$$E_r(z) = z_l\left[\frac{z^2}{2(1+\nu)}\frac{z^2 + a_1 z + a_2}{z^2 + b_1 z + b_2}\frac{e^{-z}}{z} + \left(3 + \frac{1}{2(1+\nu)}\right)[1 - e^{-z}(z+1)]\right], \quad (38)$$

where $z_l \equiv 2q_l l_c/(\pi L_f)$ and q is replaced by q_l, that is,

$$q_l = \frac{q_c}{2}\left(\frac{q}{q_c} - 1 - \frac{0.55}{a} + \sqrt{(1 + \frac{0.55}{a} - \frac{q}{q_c})^2 - 4(\frac{1}{a} - \frac{q}{q_c})}\right). \quad (39)$$

This equation (39) is the simplest expression that interpolates between the known limiting values, *i.e.* $q_l = 0$ at $q = q_c$ and $q_l \to (q - 0.55q_c)$ in the limit when both q_l and q approach infinity. The purpose of this transformation is to take into account that the network is not connected below the critical percolation density, and the contribution of the undeformed segments at the ends of the fibres above the critical percolation density. With this replacement E_e vanishes at $q = q_c/a$, as it should.

Comparing two-dimensional random fibre networks with the three-dimensional ones projected to two dimensions, we find that they are similar with one exception, the degree of bonding is lower for the projections of the three-dimensional networks, see Fig. 7. This is rather trivial since the thickness dimension prevents some of the fibres to come in contact with each other. In [II] we show that Eqs. (37) and (38) can be used to calculate the stiffness of a three dimensional random fibre network using the bonding fraction a as a matching parameter. a is now the fraction of the number of bonded contacts in the two-dimensional projection of a three-dimensional network divided by the number of contacts in the two-dimensional network of otherwise the same parameters. The model works provided that the bending angle ϕ is small, and the fraction of the bonded segments exceeds 25%, that is, $a \geq 0.25$. The second limitation comes from the fact that in three dimensions a fibre must have at least two contacts, and that connected fibres must percolate, which generates high correlations for low bonding fractions. The analytical model assumes the bonding fraction to be uniform, *i.e.* uncorrelated, across the system. This induces an upper limit for the fibre density since for large densities the bonding

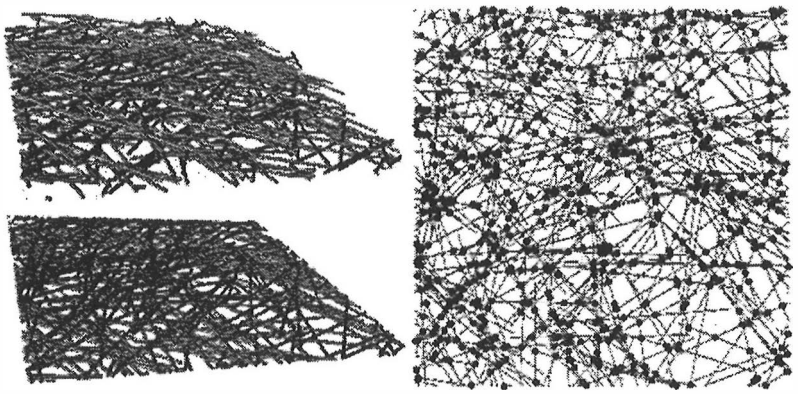

Figure 7: A three-dimensional random fibre network (left up) with $q/q_c = 7.0$, $L_f = 1.0$, $w = 0.2$ and $\phi = 0.1rad$, and its projection into two dimensions (left down). The degree of bonding is described on the right where the bonded crossings of the projection are expressed as circles: 18% of the crossings in the projection are bonded ($a = 0.18$).

fraction tends to decrease. The fibre density is also limited from below since close to the percolation limit the network becomes too sparse to be modelled using a mean-field approch. Comparing the number of bonded crossings in two-dimensional projections of three-dimensional networks, and the two-dimensional networks, we find that the fraction of bonded segments takes the form [II]

$$a = f\left(\frac{w}{w_0 \sin\phi}\right)/q, \tag{40}$$

where the function of f is not analytically known and w_0 is a suitable dimension, which we chose here to be $1m$. Changing w and ϕ so that the ratio $w/(w_0 \sin\phi)$ remains constant, is equivalent to a length scale transformation in the thickness direction of the mat, and a does not change. Solving for f numerically, see Fig. 9 and [III], gives

$$\begin{aligned} f(x) &\propto x^{-3/4}, x \lesssim 0.3 \\ f(x) &= \text{constant}, x \gtrsim 0.3. \end{aligned} \tag{41}$$

3.4.2 Porosity

We can define the areal porosity of the cross sections of a three-dimensional random fibre mat as the fraction of the cross section not covered by fibres [III] Near the substrate where the fibres lie flat, the areal porosity takes its lowest value, while near the rough upper surface region, the porosity is increased from its bulk value. This behaviour can be seen in Fig. 8, where the different lines represent different fibre densities q. In the bulk region, the areal porosity is given by

$$\epsilon_a = 1 - g\left(\frac{w}{w_0 \sin\phi}\right)\frac{w^2}{L_x L_y \sin\phi}, \tag{42}$$

where $w^2/\sin\phi$ is the area covered in the cross-section by a single fibre segment, and the function g describes the number of segments going through the cross section. The functions g and f turn out to be related through

$$f\left(\frac{w}{w_0 \sin\phi}\right) = c_1 \frac{w}{w_0 \sin\phi} g\left(c_2 \frac{w}{w_0 \sin\phi}\right), \tag{43}$$

where $c_1 = 0.2$ and $c_2 = 0.7$ are solved numerically [III] see Fig. 9. This means that we can relate the porosity of the fibre mats to the number of contacts per fibre f through the relation

$$\epsilon_a = 1 - \frac{c_2}{c_1}\frac{w_0 w}{L_x L_y} f\left(\frac{1}{c_2}\frac{w}{w_0 \sin\phi}\right). \tag{44}$$

The process function f that appears in Eqs. (37), (38), (40) and (41) through the fraction of bonding a, seems to determine the entire structure and mechanical behaviour of the fibre mats.

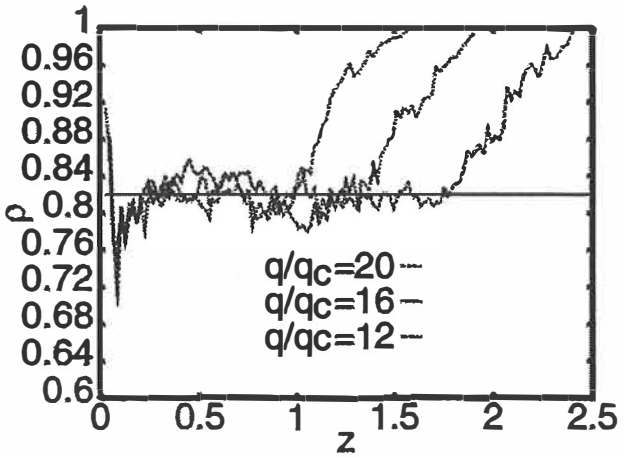

Figure 8: The plane porosity ρ as a function of mat thickness z for $q/q_c = 12$, $q/q_c = 16$ and $q/q_c = 20$. The peak on the left is the result of the fibres lying flat on the substrate and should be discarded [III].

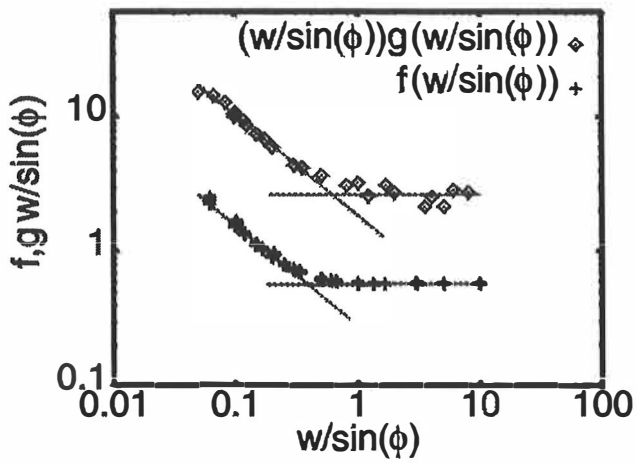

Figure 9: f and $gw/\sin\phi$ as functions of $w/\sin\phi$. For small $w/\sin\phi$ the power-law $(w/\sin\phi)^{-3/4}$ is fitted to the data. For large $w/\sin\phi$ the power-law changes to a constant value with the cross-over approximately at $w/\sin\phi = 0.3$ [III].

4 Woven fibre networks

4.1 Brief review

Machine made woven fabrics are extensively used for many purposes. Search for their optimal structure with respect to different end uses has induced a large amount of experimental work. There exists no easy way to estimate for example the elastic properties, heat conduction or fluid permeability of a multilayer fabric. Traditionally the optimisation process has incorporated manufacturing test samples followed by analysis of their properties. As the machinery is designed for fast production and not for frequent changes in the fabric structure, product development has been tedious and expensive.

4.2 Numerical model

Woven fabrics are constructed by periodically repeating a basic unit in the plane of the fabric. It is therefore sufficient to find the equilibrium configuration of the basic unit under periodic boundary conditions.

The fibres are modelled as straight lines between the nodal points where the fibres may be abruptly bent. The nodal points represent the points of contact between different fibres. The radii of the fibres enter the model in the identification of the contact locations where the fibres are prevented from penetrating each other. The nodes are therefore grouped in pairs, one node per fibre per contact, the sum of the two fibres' radii apart.

The initial configuration is such that the cross-directional fibres are straight across the unit and the longitudal fibres are woven around them in the desired configuration. Stress is introduced to the system by pulling on the segments at the (periodic) boundaries. The stress is then carried into the network along the nearest neighbour segments. The relaxation procedure is realised by the conjugate gradient method, and is explained in Section 2.5.2 and in the references [IV, V].

The fibre stiffness is assumed to depend only on the axial stretch mode, axial tension being proportional to $E_n r_n^2 \epsilon_n$, where E_n, r_n and ϵ_n are the Young's modulus, the radius and the strain of segment n, respectively. The bending stiffness of the fibres can be neglected, since fibres with large bending stiffness would almost certainly result in weave manufacturing problems, making the process either highly energy consuming or simply inducing frequent fibre breakage. As friction would lead to an infinite number of metastable equilibrium configurations, the fibres are also assumed frictionless. This is again applicable since large friction forces would badly hinder the manufacturing process.

The global energy is assumed to be found when the movement induced in the network by the pulling method is below some given threshold value. The model developed in [IV, V] is a tool for generating virtual fabric structures. These structures can then be tested with various simulation tools for their properties. An example of a computer generated fabric is shown in Fig. 10.

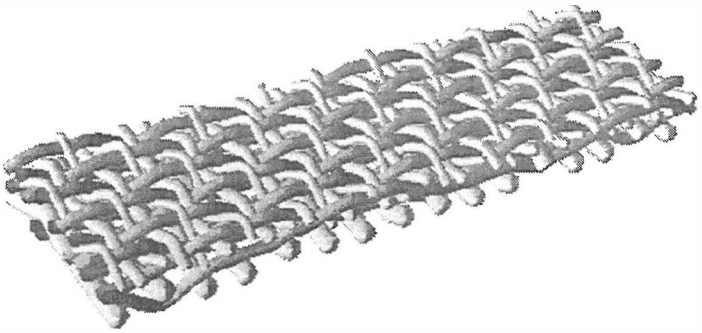

Figure 10: A computer generated woven structure.

4.3 Results

The numerical model was tested against the available real fabric structures. Because of the lack of any instruments to measure the interior of real fabrics, the virtual structures were visually compared against the cross-sections of the basic unit of the real sample.

This comparison shows good agreement between the real and simulated structures, as shown in [IV, V] and in Figs. 11-13. The model can be used to study *e.g.* the transport properties of woven structures. We are currently implementing the Lattice Boltzmann method to extract the permeability of the geometries generated using the model described.

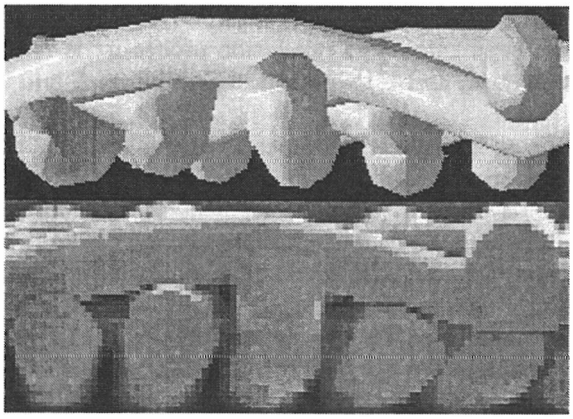

Figure 11: A side view comparison of a woven structure of 10 fibers with the the model on top and the real sample below.

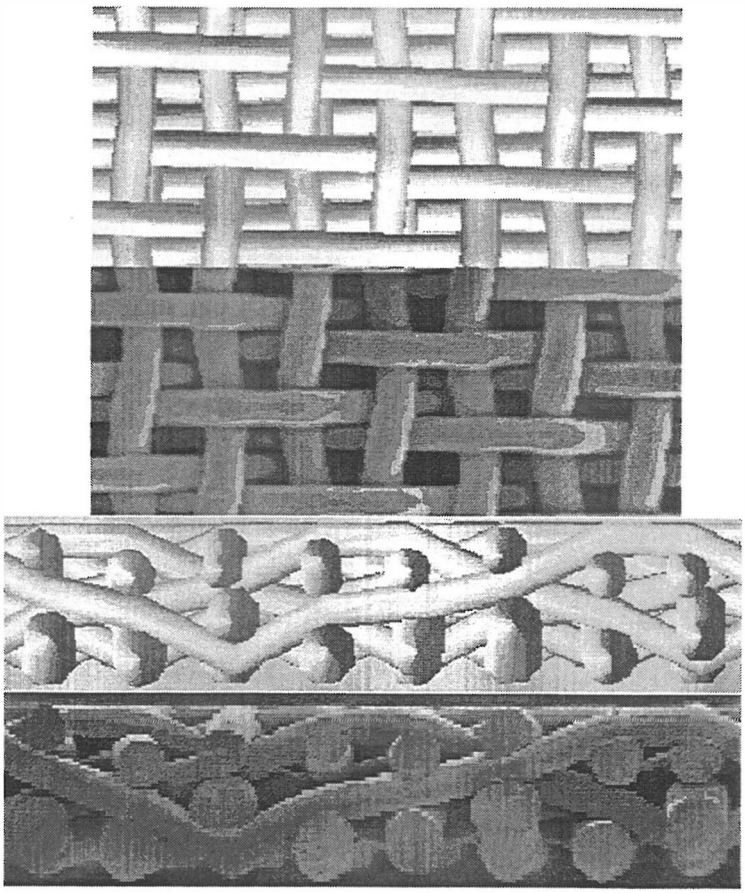

Figure 12: Comparison in two directions of a woven structure of 24 fibers with the the model on top and the real sample below.

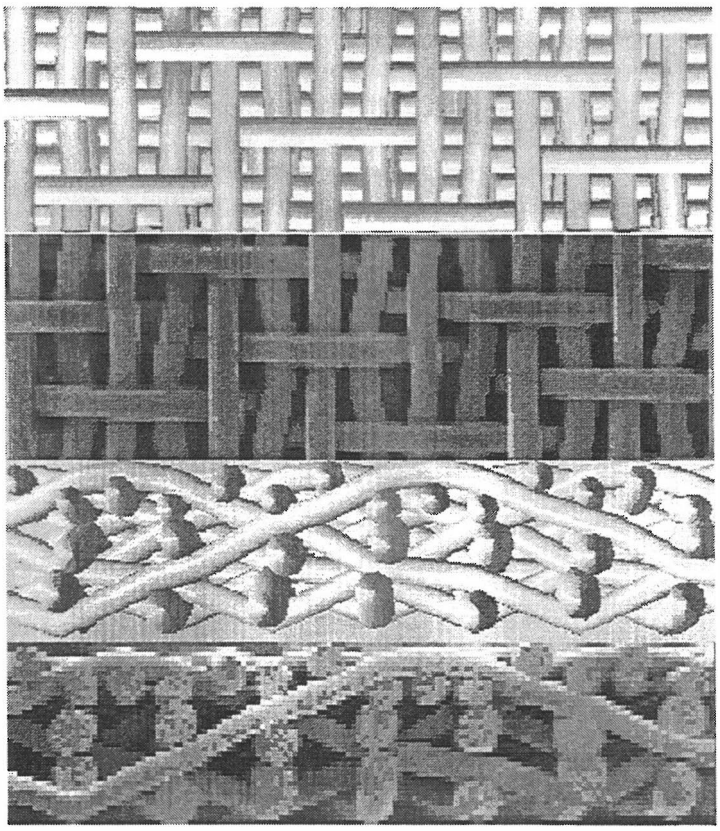

Figure 13: Comparison in two directions of a woven structure of 40 fibers with the the model on top and the real sample below.

5 Discussion

The analytical model developed for the stiffness of the random fibre networks is a powerful tool for analysing fibrous structures. The in-plane stiffness of a random fibre structure can be extracted, if we know the properties of the building blocks of the system. These properties are often well known and the model can be used to optimise a system by altering the building blocks. This was done *e.g.* in Ref. [II] to draw information about how the bending angles of the fibres affect the tensile stiffness of the network.

The connection between two-dimensional and three-dimensional structures [II] opens up a possibility to exploit two-dimensional images in analysing three-dimensional structures. The only parameter needed in addition to the properties of the building blocks is the fraction of bonding of the building blocks in contact. This applies also to the porosity of the system as the properties needed are the fibre width and the bending angle, albeit the analytical form of the process function is not yet known.

As the process function [III] seems to determine the entire structure and mechanical behaviour of the fibre mats, the effective-medium theory developed, together with the simulation model, offer a solid platform for future development in the analysis of geometrical and mechanical properties of materials with random connections.

In woven fibrous structures the model presented in this thesis for relaxing a network with multiple boundary conditions, has proved to be an excellent approach due to its intuitive simplicity and to the computing power needed. The assumptions made concerning the vanishing bending stiffness and friction, are in accordance with the manufacturing process of real fabrics. As the numerical model incorporates a specific case of the gradient method, it falls into a category of modern numerical methods that are currently being developed and used on a wide basis. The model can be extended into more elaborate cases by modifying the contacts such that plasticity and friction are taken into account.

References

[1] N. E. Cusack, The Physics of Structurally Disordered Matter: An introduction, IOP Publishing Ltd, Bristol (1987)

[2] G. E. Pike and C. H. Seager, Phys. Rev. B **10**, 1421 (1974)

[3] I. Balberg and N. Binenbaum, Phys. Rev. B **28**, 3799 (1983)

[4] F. Carmona, F. Barreau, R. Canet, and P. Delhaes, J. Phys. (France) **41**, 534 (1980)

[5] H. Herrman and S. Roux (eds.), Statistical models for the fracture of disordered media, North-Holland, Amsterdam (1990)

[6] R. C. Hamlen, Paper structure, mechanics, and permeability: Computer-aided modeling. Ph.D. thesis, University of Minnesota, USA (1991)

[7] S. Heyden, A network model applied to cellulose fibre materials, licenciate thesis, Lund Institute of Technology, Report TVSM-3018 (1996)

[8] J. M. Ziman, Models of disorder, Theoretical physics of homogeneously disordered systems. Cambridge University Press, Oxford (1971)

[9] L. D. Landau and E. M. Lifshitz, Theory of Elasticity, Pergamon Press, Exeter (1970)

[10] E. Pennala, Lujuusopin perusteet, Otakustantamo 407, Helsinki (1990)

[11] G. Strang and G. J. Fix, An Analysis of the Finite Element Method, Prentice-Hall, Englewood Cliffs, N.J. (1973)

[12] H. Kardestuncer, Finite Element Handbook, McGraw-Hill, New York (1987)

[13] A. Samuelsson and N.- E. Wiberg, Finite Element Method Basics, Studenlitteratur, Lund (1998)

[14] M. Hakala, Elementtimenetelmä lujuusopissa, Otakustantamo 457, Espoo (1982)

[15] C. Johnson, Numerical Solution of Partial Differential Equations by the Finite Element Method, Studentlitteratur, Lund (1987)

[16] S. C. Brenner and L. R. Scott, The Mathematical Theory of Finite Element Methods, Springer, New York (1994)

[17] Modelling and computing in industry, Lecture notes, Center for Scientific Computing, Espoo (1999)

[18] G. H. Golub, C. F. van Loan, Matrix Computations, North Oxford Academic, Oxford, (1986)

[19] S. Pissanetzky, Sparse Matrix Technology, Academic Press, London (1984)

[20] A. George, J. W. Liu, Computer Solution of Large Sparse Positive Definite Systems, Prentice-Hall, Englewood Cliffs, N.J. (1981)

[21] R. Barret *et al*, Templates for the Solution of Linear Systems, SIAM, Philadelphia (1993)

[22] A. Greenbaum, Iterative Methods for Solving Linear Systems, SIAM, Philadelphia (1997)

[23] H. Voss, Iterative Methods for Linear Systems of Equations, Lecture notes of The 3rd International Summer School, Jyväskylä, Finland (1993)

[24] W. H. Press, *et al*, Numerical Recipes in Fortran: The Art of Scientific Computing, Cambridge University Press, Cambridge (1989)

[25] W. H. Press, W. T. Vetterling, S. A. Teukolsky, B. P. Flannery. Numerical Recipes in Fortran 90: The Art of Scientific Computing, Cambridge University Press, New York (1996)

[26] Numerical Alrogithms Group, Ltd. http://www.nag.co.uk/

[27] Visual Numerics, http://www.vni.com/index.html

[28] ITPACK-library, http://www.ma.utexas.edu/CNA/ITPACK/

[29] HSL - Harwell Subroutine Library, http://www.cse.clrc.ac.uk/Activity/HSL

[30] J.Åström, M. Kellomäki and J. Timonen, Elastic waves in random-fibre networks, Journal of Physics A **30**, 6601 (1997)

[31] J.Åström, M. Kellomäki, M. Alava and J. Timonen, Propagation and kinetic roughening of wave fronts in disordered lattices, Phys. Rev. E **56**, 6042 (1997)

[32] M. Kellomäki, J. Åström and J. Timonen, Early-time dynamics of wave fronts in disordered triangular lattices, Phys. Rev. E **57**, R1255 (1998)

[33] M. Kellomäki, J. Åström and J. Timonen, Elastic-wave fronts in one- and two-dimensional random media, to be published

[34] M. Kellomäki, J. Åström and J. Timonen, Rigidity and dynamics of random spring networks, Phys. Rev. Lett. **77**, 2730 (1996)

[35] D. J. Jacobs, M. F. Thorpe, Generic rigidity percolation: The pebble game, Phys. Rev. Lett. **75**, 4051 (1995)

[36] S. P. Obukhov, First order rigidity transition in random rod networks, Phys. Rev. Lett. **74**, 4472 (1995)

[37] J. Åström, M. Alava and J. Timonen, Crack dynamics and surfaces in elastic beam lattices, Phys. Rev. E **57**, R1259 (1998)

[38] J. Åström, M. Alava and J. Timonen, Roughening of a propagating planar crack front, Phys. Rev. E **62**, 2878 (2000)

[39] M. Rigdahl, B. Westerlind, H. Hollmark, Analysis of cellulose networks by the finite element method. Journal of Materials Science, vol 19, pp 3945-3952

[40] H. L. Cox, Br. J. Appl. Phys. **3**, 72 (1952)

[41] D. H. Page and R. S. Seth, Tappi J. **63**, 113 (1980)

[42] V. I. Räisänen, M. J. Alava, K. J. Niskanen and R. M. Nieminen, J. Mater. Res. **12**, 2725 (1997)

[43] J. Åström, S. Saarinen, K. Niskanen and J. Kurkijärvi, J. Appl. Phys. **75** 2383 (1994)

[44] J. A. Åström and K. J. Niskanen, Europhys. Lett. **21**, 557 (1993)

[45] M. Kimura and H. Uchimura, Sen'i Gakkaishi **51**, 550 (1995)

[46] M. Murat, M. Anholt and H. D. Wagner, J. Mater. Res. **7**, 3120 (1992)

[47] L. Monette, M. P. anderson and G. S. Grest, J. Appl. Phys. **75**, 1155 (1994)

Appendix: Included publications

I Elasticity of Poissonian Fiber Networks
J.A. Åström, J.P. Mäkinen, M.J. Alava, and J. Timonen
Phys. Rev. E **61**, 5550 (2000)
https://doi.org/10.1103/PhysRevE.61.5550

Ia Erratum: Elasticity of Poissonian Fiber Networks
J.A. Åström, J.P. Mäkinen, M.J. Alava, and J. Timonen
Phys. Rev. E **62**, 5862 (2000)
https://doi.org/10.1103/PhysRevE.62.5862

II Stiffness of Compressed Fiber Mats
J.A. Åström, J.P. Mäkinen, H. Hirvonen and J. Timonen
J. Appl. Phys. **88**, 5056 (2000)
https://doi.org/10.1063/1.1315622

III Elasticity and Porosity of Three Dimensional Mats of Randomly Deposited Fibers
J.P. Mäkinen, J.A. Åström, S. Kähkönen and J. Timonen
Submitted.
https://doi.org/10.1007/s10035-003-0131-0

IV Modeling Multilayer Woven Fabrics
J.A. Åström, J.P. Mäkinen, and J. Timonen
Submitted.
https://doi.org/10.1063/1.1385350

V A Relaxation Model for Multi-Layered Woven Fabrics
J.P. Mäkinen, J.A. Åström and J. Timonen
Proceedings of ECCOMAS 2000 (2000)

V

European Congress on Computational Methods in Applied Sciences and Engineering
ECCOMAS 2000
Barcelona, 11-14 September 2000

A RELAXATION MODEL FOR MULTI-LAYERED WOVEN FABRICS

J.P. Mäkinen*, J.A. Åström†, and J. Timonen‡

*Department of Physics, University of Jyväskylä, P.O.box 35, FIN-40351 Jyväskylä, Finland; email: jukka.makinen@phys.jyu.fi, web page: http://www.phys.jyu.fi/homepages/jupemak

†Department of Physics, University of Jyväskylä, P.O.box 35, FIN-40351 Jyväskylä, Finland; email: astrom@phys.jyu.fi

‡Department of Physics, University of Jyväskylä, P.O.box 35, FIN-40351 Jyväskylä, Finland; email: jussi.timonen@phys.jyu.fi, web page: http://www.phys.jyu.fi/homepages/timonen

Key words: relaxation, fabric, hard-core, contact

Abstract. *A model for the relaxation of large woven networks to the minima of their elastic energies is introduced. The load in the system is carried by fibre segments between the contacts that are considered frictionless. During the relaxation process contacts are formed and opened as the system moves towards its energy minimum. The model introduces a new solution method for the relaxation of systems with multiple hard-core contacts.*

1 INTRODUCTION

Woven fabrics of various kinds are typical everyday materials but also play an important role in many industrial processes. Modelling has not been applied, however, to the design of materials of this kind. The related industries have traditionally not had a need to apply advanced technologies. This situation is now changing: increasingly more sophisticated properties for materials of also this kind are required. In order to meet their end-use requirements, more complicated structures are needed, and modelling is becoming an important tool in their design. The traditional trial and error method of design is rather costly and time consuming.

Physically realistic modelling of woven fabrics is not however an easy task. Relaxation of a network of fibres towards its equilibrium configuration involves formation of new and opening of existing contacts between fibres. This makes the problem nonlinear. The related dynamics, which is similar to hard-core dynamics, has been difficult to realise in previous applications. We have now created an algorithm which can produce a woven structure of desired design with very few real restrictions. We use a limited number of contraints that arise from the practical application we have in mind, but most them could be lifted. In the relaxation method a few simplifying assumptions were also made, mainly for computational efficiency as we want, at the moment, to avoid long computing times.

2 THE MODEL

A woven fabric usually consists of a basic unit which is copied in every direction to form the textile. It is therefore enough to model the basic unit with periodic boundary conditions.

The model consists of fibres represented as one-dimensional piecewise linear nearest neighbour links. The radii of the fibres enter the model in the identification of contacts when the segments are prevented from penetrating each others. The fabric as a whole then consists of a nearest neighbour network of nodes connected with one-dimensional segments.

The nodes on a fibre can be classified as single or double. By a double node we mean a point where two fibres are in contact, i.e. they "collide", so that there are four segments that meet at a node of this kind. A single node is just a consequence of piecewise linearity of the fibres: they can bend at nodes of this kind. Thus there are only two segments that meet at a single node.

In the initial configuration of the network the cross-directional fibres go straight across the unit, and the longitudal fibres are woven around them in the desired configuration. Stress is introduced to the network by pulling on the segments at the (periodic) boundaries. The stress is then carried along the nearest neighbour segments into the network.

The local energy minimum of the network is sought by moving the nodes along the resultant force vectors applied on them. The force vectors are generated by summing up the tension vectors of the segments attached to the nodes. As the nodes are moving, the

possible collisions of the segments with other segments in the network are monitored. On collision a new contact, i.e. a new double node, is formed between the colliding segments. The distance of the two nodes of a contact is given by the sum of the radii of the colliding fibres and is kept constant throughout the lifetime of the contact. In this sense our networks are hard-core systems.

For a contact, i.e. a double node, the resultant force vector is found by summing up the force vectors of the two nodes. The contact is then moved along the the resultant force vector.

If the force vectors on the two nodes of a contact point in opposite directions, the contact is pulled apart. The resulting two single nodes are then moved along their respective force vectors. If the force vector on a single node vanishes, the node is removed and the adjacent nodes are connected with a single segment.

The motion vector of a contact is of the form

$$\vec{p} = f\vec{s}, \tag{1}$$

where

$$\vec{s} = \sum_{neighbours} \hat{l}_n t_n. \tag{2}$$

Here $\hat{l}_n$ is a unit vector at the node in the direction of its n^{th} neighbour, and t_n the tension at the n^{th} neighbouring segment.

The parameter f in the equation is a relaxation parameter which is chosen such as to ensure rapid convergence. Too small an f will increase the relaxation time whereas if f is too large, unwanted oscillations will be generated.

There is no friction in the system as the contacts slide freely along the fibres. Moreover no bending stiffness of the fibres is accounted for. If needed the method easily allows a harder pull at the boundaries on fibres with larger bending stiffnesses as this effectively makes the fibres straighter in the relaxed state. As bending a fibre also means stretching it we can deduce from the Hooke's law that the extra pull at the boundaries would be of the form [1]

$$F \propto Er^2, \tag{3}$$

where E and r are the Young's modulus and the radius of the fibre, respectively.

In addition to monitoring the segment collisions, it is necessary to prevent the nodes from penetrating the segments. This is done simply by blocking the node. No new contacts are formed in node to segment collisions.

The global energy of the network is minimised by going through the nodes iteratively. When the length of the largest motion of a node in the network is below some value $p_{relaxed}$, the global energy minimum is assumed to be found.

3 COMPARISON WITH EXPERIMENTS

Some networks generated by the pull-detect method described above were compared with real woven-fabric configurations of the same design. The fibres used in the fabrics

were made of plastic with a relatively low friction coefficient so that the assumption of non-frictional fabric used in the relaxation should be quite well satisfied. At this point we do not perform a quantitative comparison of the real and model structures, but are satisfied with a qualitative visual inspection. It is evident from figs. 1 and 2 that modelling can produce very realistic configurations.

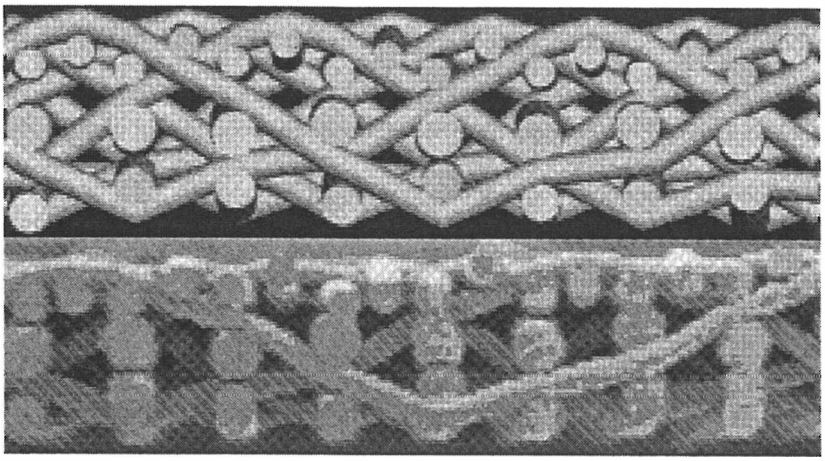

Figure 1: A side-view comparison between the model (upper) and a real woven fabric (lower) in the relaxed state. The basic unit contains 32 cross-directional fibres in three layers and eight longitudal fibres.

The computer used in the modelling was a Pentium II - 400 Mhz laptop with 128MB of on-board memory. For every configuration tested the relaxation time was on the scale of a few minutes.

4 DISCUSSION

The need for constant development of industrial textiles may lead to a cycle of trials and errors which is often expensive and time consuming. The test samples have to be manufactured and analysed, and in the worst case the whole assembly line would be out of production during this time. Still at the end of testing the results may well be disappointing.

To date this has been in practice almost the only way of developing textiles. In the basic unit of a fabric, which is periodically copied in the lateral directions, the number of fibres may well be ten times thirty in four layers. Finding the global energy minimum of the system includes a minimisation of a highly nonlinear elastic problem. This means finding the minimum energy configuration for every fibre in the presence of the several boundary conditions set by the other fibres. The global energy function of the system is very complex. Contacts between the fibres are hard-core which usually are very difficult

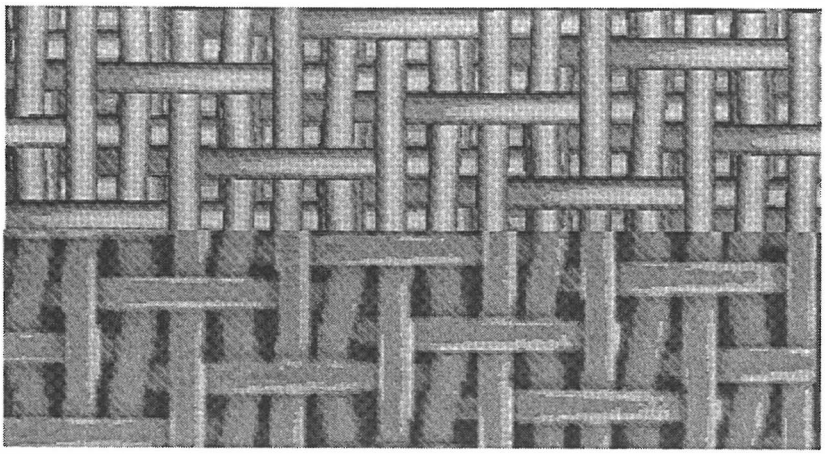

Figure 2: A comparison between the top views of the same fabric configuration. The upper picture is again the model and the lower picture the real fabric. We suspect that the difference seen here follows from the non-frictional modelling of the threads.

to handle, and the fibres may come in contact with nearly every other fibre in the system. Solving the problem with standard methods would have been very time consuming.

The method we use includes hard-core contact handling with a very fast iterative search for the global elastic equilibrium. The method does not require much memory in its data structures, and is very fast with convergence times of the order of a few minutes for all the relevant cases we have studied. This ensures the use of the method without large investments on computer power. The output of the method is the geometrical structure of the fabric in terms of nodal co-ordinates. This information can be further analysed with other computational methods. These include different stiffness modes using the conjugate gradient method, flow of water through the fabric using the lattice-Boltzmann method, and several geometrical properties of the system, just to mention a few.

REFERENCES

[1] L. D. Landau and E. M. Lifshitz Theory of Elasticity, Pergamon Press, Great Britain, 1970.